Theoretical study of the high pressure effect in the crystalline structure and properties of the indium selenide.

FINAL DEGREE PROYECT

Author: Sergio Alcalde Castillo

Tutor: Armando Beltran Flors

Physics and Analytics department

Castellón, 12/7/2019

Aim

The aim of this project is the theoretical study, using Crystal software, of the R3m (α) and P61 (γ) In_2Se_3 phases stability and properties under pressure.

Introduction:

The two structures that are going to be studied are shown below, jointly with their properties and different uses.

α-In_2Se_3 (R3m)

Properties:
For the compound α-In2Se3, trigonal or R3m (Figure 1), may be another related structures that are not going to be studied.

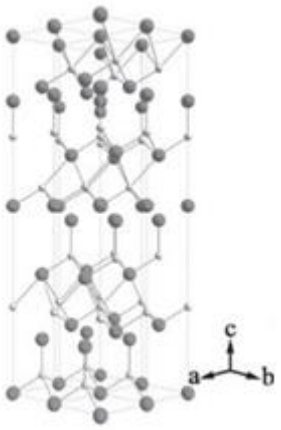

Figure 1. Alpha structure

The α-In_2Se_3 exhibits room-temperature ferroelectricity[1] with reversible spontaneous electric polarization in both out-of-plane and in-plane orientations. Its non-centrosymmetric crystalline structure leads to an intrinsic stabilization of the electric polarizations in-plane and out-of-plane, through the blockage by dipoles, which gives rise to multidirectional electrical current.

The ferroelectric properties of In_2Se_3 can provide an additional control in optoelectronic or photovoltaic applications.

It is known that In_2Se_3 single crystals with a stable phase can grow by introducing impurities during the crystal growing[2]. Therefore, an appropriate amount of certain impurities is added to a single In_2Se_3 crystal to make In_2Se_3 single crystals grow, with a stable alpha phase and a high grade of electric conductivity and mobility, but with the optical properties of a pure crystal. To obtain these crystals, the bases and impurities of SiO_2 (as a crystal layer) were studied, and also the formation when Indium is present.

Uses:

The compound α-In_2Se_3 with a layer structure is an excellent material with applications in solar cells and ionic batteries and several studies about their optical and electric properties have been published[3].

A solar, or photovoltaic, cell is an electric device that transforms the light energy directly into electricity by photovoltaic effect, which is a physical and chemical phenomenon. It is a sort of photoelectric cell, defined as a device whose electrical characteristics, such as current, voltage or resistance, change when exposed to light. The devices of individual solar cells can be combined to make modulus, also known as solar panels.

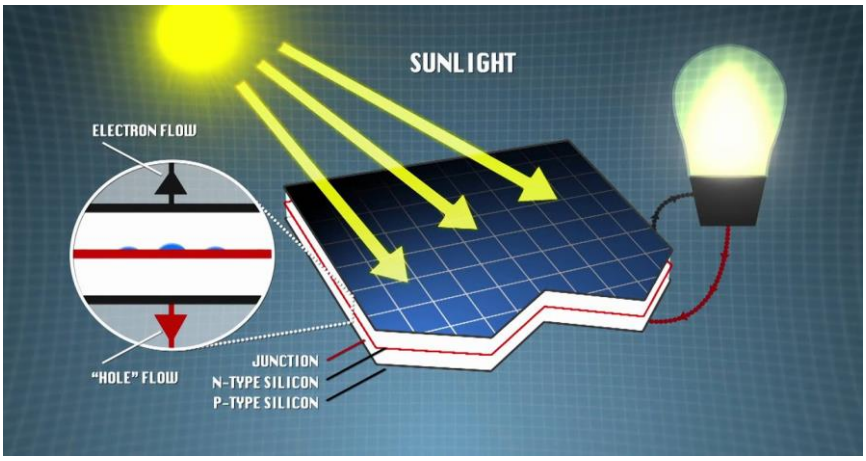

Figure 2.Example of photovoltaic cell

Ionic battery is a device designed for electrical energy storage that uses a salt as electrolyte, to get the necessary ions for the reversible chemical reaction taking place between cathode and anode.

The properties of the batteries, such as lightness of their components, high energetic capacity and resistance to be discharged, together with the low memory effect they suffer, or their capacity to work out high number of regeneration cycles, have allowed to design light weight accumulators, of small size and varied shapes, with a high yield, specially adapted to the applications of electronic industry of high consumption.

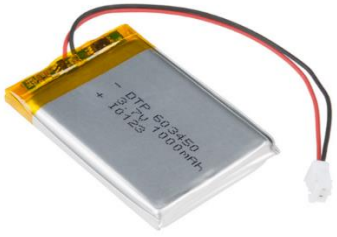

Figure 3.Lithium ionic battery

γ-In_2Se_3 (P61- spg 169)

Properties:

Until now, low attention was paid to γ-In_2Se_3. In this phase obtained at high temperature, the vacancies are not organised in planes bur ordered along c axis in a helicoidally form.

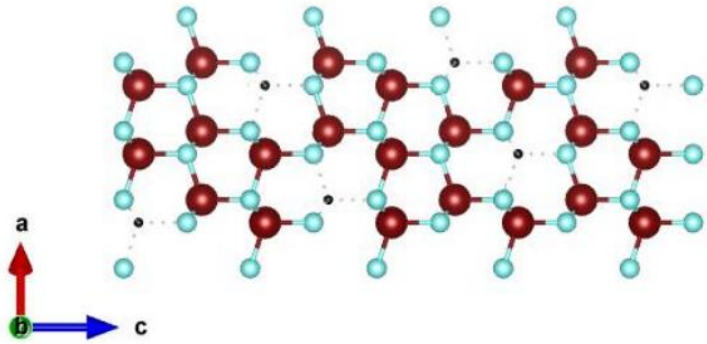

Figure 4. Gamma structure

Currently the researchers are focusing in the unidimensional γ-In_2Se_3 nanostructure[4], since it may show an excellent light absorption due to its high surface/volume ratio.

Uses:

It is used as part of the solar cells. The γ-In_2Se_3 requires the deposition in different substrates with a high crystalline quality. It is known that Si can be a good substrate to cultivate nanostructures because it offers a lot of advantages, such as good doping properties and thermal conductivity. If the Si substrate can be used for the growing of nano-γ-In_2Se_3, several integrated circuit devices based on Si could be developed in future[5].

Calculation Methods:

Hartree-Fock Method.

First, it is interesting to explain that method required that the final computed field from the charge distribution to be "self-consistent" with the assumed initial field. Therefore the self-consistency was a requirement of the solution and hence the name.

That said, the Hartree-Fock (HF) method used in Chemistry is an approximation method to determine or solve the wave function and the energy of many bodies interacting in the stationary phase (complying with Eq. 1) that is time independent.

$$|\Psi(\mathbf{r},t)|^2 = \Psi^*(\mathbf{r},t)\Psi(\mathbf{r},t) = \psi^*(\mathbf{r})e^{iEt/\hbar}\psi(\mathbf{r})e^{-iEt/\hbar} = \psi^*(\mathbf{r})\psi(\mathbf{r}) = |\psi(\mathbf{r})|^2$$

Eq.1

This method was developed by D.R. Hartree in 1927, a bit after the discovery of Schrödinger's equation. It is based on semi-empiric methods established by Bohr, such as the calculation of the energy of one state - for the Hydrogen atom - that is related with the main quantum number in the following way:

$$E = -1/n^2$$

Eq.2

Starting from this equation, the energy levels of multi-electronic atoms may be defined when taking into account that the shielding of inner electrons is not total and, then, there is a quantum defect (d). Doing this, the formula for the energy levels is approximated with the following one:

$$E = -1/(n+d)^2$$

Eq.3

Once the equation is developed, it is considered that the whole nucleus is fixed with the exception of the electrons (Eq. 4) and a potential V is generated by the Born-Oppenheimer approximation that is considered as reference. Thus, this method uses a self-consistent potential (each electron moves in a potential created by the rest of the electrons) to convert a multi-electronic problem into multiple mono-electronic problems. In this way the Schrödinger's equation of one atom electronic state for N electrons per atom is got (Eq. 5).

$$\Psi_{\text{total}} = \psi_{\text{electronic}} \otimes \psi_{\text{nuclear}}$$

Eq.4

$$\hat{H}\Psi = \left[\widehat{Kin} + \hat{V} + \widehat{Rr}\right]\Psi = \left[\sum_{i}^{N} -\frac{\hbar^2}{2\,m}\nabla_i^2 + \sum_{i}^{N} V\,(\vec{r}_i) + \sum_{i<j}^{N} Rr(\vec{r}_i,\vec{r}_j)\right]\Psi = E\,\Psi$$

Eq.5

The analytic solution for this equation has not been found because the term $\widehat{Rr}$ depends as much from the electron i as from the electron j.

Another consideration performed when applying this method is that each solution is a linear combination of a finite number of base functions and, moreover, that each self-function is described by Slater's determinant, which for a system of N electrons is defined as:

$$\Psi(\mathbf{x}_1, \mathbf{x}_2, \ldots, \mathbf{x}_N) = \frac{1}{\sqrt{N!}}\begin{vmatrix} \chi_1(\mathbf{x}_1) & \chi_2(\mathbf{x}_1) & \cdots & \chi_N(\mathbf{x}_1) \\ \chi_1(\mathbf{x}_2) & \chi_2(\mathbf{x}_2) & \cdots & \chi_N(\mathbf{x}_2) \\ \vdots & \vdots & \ddots & \vdots \\ \chi_1(\mathbf{x}_N) & \chi_2(\mathbf{x}_N) & \cdots & \chi_N(\mathbf{x}_N) \end{vmatrix}$$

Eq.6

Thanks to this determinant, the following considerations are met:

- The result will be an anti-symmetric function and, therefore, the symmetric ones will be disregarded.
- Pauli's exclusion laws compliance is assured.

In theory to use Slater's determinant as the approximation of the electronic wave function is correct, but the exact wave functions cannot be expressed by means of this determinant, since the Coulombic correlation is not taken into account. Therefore a different result to the exact solution of the Schrödinger's equation with the Born-Oppenheimer's approximation will be obtained and the difference between both will be the correlation energy.

Finally, to indicate that this method is solved by convergence with an iterative methodology that is the following one:

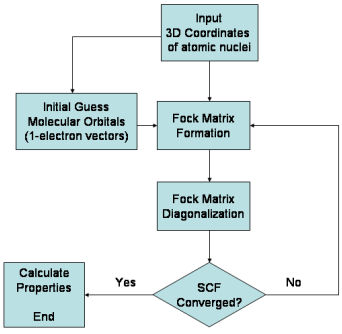

Figure 5. Simplified algorithmic flowchart illustrating the Hartree–Fock method

As a summary of this method:

1. Born-Oppenheimer's approximation is considered.

2. Relativistic effects are not taken into account.

3. It is assumed that the variational solution is the linear combination of a finite number of base functions.

4. Slater's determinant is considered as the description of each self-function energy.

5. The coulombic correlations are not taken into account for electrons with opposite spins, but they are for the ones with parallel spins.

Density Functional Theory (DFT)

It is a variational quantum-mechanical computational model, used to study the electronic structure, principally the basic state, of many-body systems (in this Project a multi-electronic compound is addressed). This model was started to be developed by L. Thomas and E. Fermi but the calculations were not established finally until 40 years afterwards, with P. Hohonberg, W. Kohn y L. Sham. It is presented as an alternative to the Schrödinger's equation solution and solved by means of the electronic energy minimisation versus the electronic density.

The use of the electronic density versus the wave function makes it simpler and thus accessible to solve more complex systems since, instead of having 3N variables (in the case of the wave function), only 3 variables are present.

What is got with this method is, starting from a dependent on $\widehat{Rr}$ many-body problem, to get a non-dependent on $\widehat{Rr}$ single-body problem. In order to do it, the key variable is the electron density (n), which for a normalised Ψ is:

$$n(\vec{r}) = N \int \mathrm{d}^3 r_2 \cdots \int \mathrm{d}^3 r_N \, \Psi^* (\vec{r}, \vec{r}_2, \ldots, \vec{r}_N) \, \Psi (\vec{r}, \vec{r}_2, \ldots, \vec{r}_N) .$$

Eq. 7

This relationship can be reverted, which implies that for a given basic state density $n_0(\vec{r})$ there is a basic state wave function.

$$\Psi_0 = (\overrightarrow{\mathrm{r}_1}, \ldots, \overrightarrow{\mathrm{r}_\mathrm{N}}).$$

Eq. 8

So Ψ_0 is an only functional of n_0.

$$\Psi_0 = \Psi[n_0]$$

Eq. 9

And consequently the value expected of the basic state of an observable $\widehat{Rr}$ is also a functional of n_0:

$$Rr[n_0] = \langle \Psi[n_0] | \widehat{Rr} | \Psi[n_0] \rangle$$

Eq. 10

In particular, the energy of the ground state is a functional of n_0

$$\mathrm{E}_0 = E[n_0] = \langle \Psi[n_0] | \hat{T} + \hat{V} + \widehat{Rr} | \Psi[\mathrm{n}_0] \rangle$$

Eq. 11

Where the contribution of the external potential $\langle \Psi[n_0] | \hat{V} | \Psi[n_0] \rangle$ can be written in terms of the density of the basic state n_0

$$V[n_0] = \int V(\vec{r}) n_0(\vec{r}) d^3r$$

Eq. 12

Therefore, the contribution of the external potential $\langle \Psi | \hat{V} | \Psi \rangle$ can be written in terms of the density n

$$V[n] = \int V(\vec{r}) n(\vec{r}) d^3r$$

Eq. 13

The functional $T[n]$ and $Rr[n]$ are the called functional universal whereas $V[n]$ is the called no universal functional, since it depends of the system studied. As soon as system specified, have to minimise the functional

$$E[n] = T[n] + Rr[n] + \int V(\vec{r}) n(\vec{r}) d^3r$$

Eq. 14

Assuming we have expressions of $T[n]$ and $Rr[n]$, the minimisation of n_0 can be carried out. The problems that may appear when minimising can be solved if Lagrange's method is applied (non-determined multipliers), where it is considered that there is no interaction electron-electron and therefore that term is eliminated remaining:

$$E_s[n] = \langle \Psi_s[n] | \hat{T}_s + \hat{V}_s | \Psi_s[n] \rangle$$

Eq. 15

In the equation, $\hat{T}_s$ is still the kinetic energy but now taking into account no interaction. $\hat{V}_s$ is the effective external potential where the bodies move about.

If it is considered that $\boldsymbol{n_s(\vec{r}) = n(\vec{r})}$ then $\hat{V}_s$ is:

$$\hat{V}_s = \hat{V} + \widehat{Rr} + (\hat{T} + \hat{T}_s)$$

Eq. 16

With all the previous calculations and assumptions, the Kohn-Sham's equations are solved for non-interactive systems.

$$\left[-\frac{\hbar^2}{2\,m}\nabla^2 + V_s(\vec{r})\right]\varphi_i(\vec{r})$$

Eq. 17

Providing the orbital φ_i which substitutes $n(\vec{r})$ within the original system

$$n_s(\vec{r}) = n(\vec{r}) = \sum_i^N \left|\varphi_i(\vec{r})\right|^2$$

Eq. 18

In the same way as for the Hartree-Fock's method, to solve the Khon-Sham's equation a $n(\vec{r})$ is assumed. This will be the first term in the iterative method, where firstly V_s is calculated and then a new density is obtained fromV_s. The process is repeated till the results converge (which always happens, in the contrary way than in Hartree-Fock).

Comparative table of the HF and DFT methods

HF (1928, 1930)	DFT (1964, 1965) (ρ = n)
$E = E(\Psi, R_\alpha)$	$E = E(\rho, R_\alpha)$
$E = \int \Psi^* \left[\sum_i h_i + \sum_{i>j} \frac{1}{r_{ij}}\right] \Psi d\tau$	$E = T_s[\rho] + U[\rho] + E_{xc}[\rho]$
$\Psi = \lvert\Psi_1(1)\Psi_2(2),\ldots,\Psi_N(N)\rvert$	$\rho(r) = \sum_{occ} \lvert\Psi_i(r)\rvert^2$
$\partial E / \partial \Psi = 0$	$\partial E / \partial \rho = 0$
$\left[-\frac{1}{2}\nabla^2 + V_C + v_x^i(r)\right]\Psi_i = \varepsilon_i \Psi_i$	$\left[-\frac{1}{2}\nabla^2 + V_C + \mu_{xc}(r)\right]\Psi_i = \varepsilon_i \Psi_i$ com $\mu_{xc}(r) = \delta E_{xc}[\rho] / \delta\rho(r)$

Hybrid functionals

The hybrid functionals are approximations that include the theories DFT and Hartree-Fock include in a way that an increased accuracy is got in the results for atomic energies, elastic constants or vibration frequencies. It is started to be used by 1993 introduced by A. Becke.

Most of the hybrid functionals are formed by the linear combination of the exact exchange functional of Hartree-Fock E_x^{HF}:

$$E_{\mathrm{x}}^{\mathrm{HF}} = -\frac{1}{2}\sum_{i,j}\int\int \psi_i^*(\mathbf{r}_1)\psi_j^*(\mathbf{r}_2)\frac{1}{r_{12}}\psi_j(\mathbf{r}_1)\psi_i(\mathbf{r}_2)\,d\mathbf{r}_1\,d\mathbf{r}_2$$

Eq. 19

And a number of exchange and correlation explicit density functionals. The parameters that determine the weight of each individual functional are adjusted by predictions of thermodynamic data either experimental or approximated.

There are several kinds of hybrid functionals, though in this project only B3LYP y HSE06 are going to be used due to, according to the bibliography, they provide better results for the calculations that will be carried out.

- **B3LYP**[6]

The exchange-correlation functional B3LYP or Becke-3 parameters-Lee-Yang-Parr is applied using the following exchange-correlation functional:

$$E_{\mathrm{xc}}^{\mathrm{B3LYP}} = E_{\mathrm{x}}^{\mathrm{LDA}} + a_0(E_{\mathrm{x}}^{\mathrm{HF}} - E_{\mathrm{x}}^{\mathrm{LDA}}) + a_{\mathrm{x}}(E_{\mathrm{x}}^{\mathrm{GGA}} - E_{\mathrm{x}}^{\mathrm{LDA}}) + E_{\mathrm{c}}^{\mathrm{LDA}} + a_{\mathrm{c}}(E_{\mathrm{c}}^{\mathrm{GGA}} - E_{\mathrm{c}}^{\mathrm{LDA}})$$

Eq. 20

The parameters used are: $a_0 = 0.20$, $a_x = 0.72$ and $a_c = 0.81$. Additionally E_x^{GGA} and E_c^{GGA} are approximations of generalised gradients (Becke 88 exchange functional and Lee-Yang-Parr correlation functional):

$$E_{\mathrm{XC}}^{\mathrm{GGA}}\left[n_\uparrow, n_\downarrow\right] = \int \varepsilon_{\mathrm{XC}}\left(n_\uparrow, n_\downarrow, \nabla n_\uparrow, \nabla n_\downarrow\right) n(\vec{r})\,\mathrm{d}^3r.$$

Eq. 21

Lastly, the parameter E_c^{LDA} is referred to the Volsko-Wilk-Nusair's local-density approximation for the correlation functional:

$$E_{\mathrm{XC}}^{\mathrm{LDA}}[n] = \int \varepsilon_{\mathrm{XC}}(n) n(\vec{r})\,\mathrm{d}^3r.$$

Eq. 22

There are three parameters that are obtained from the precursor of this method, the B3PW91: Ionisation potentials, protonic affinity and total atomic energy.

- **HSE06**[7]

The exchange-correlation functional HSE (Heyd-Scuseria-Ernzerhof) uses the Gauss' error function applied to a shielded coulombic potential to calculate the energy exchange for improving the efficiency in the calculations:

$$E_{\mathrm{xc}}^{\omega\mathrm{PBEh}} = aE_{\mathrm{x}}^{\mathrm{HF,SR}}(\omega) + (1-a)E_{\mathrm{x}}^{\mathrm{PBE,SR}}(\omega) + E_{\mathrm{x}}^{\mathrm{PBE,LR}}(\omega) + E_{\mathrm{c}}^{\mathrm{PBE}}$$

Eq. 23

The parameters are: a (a parameter used to adjust the methods forming the HSE) with a standard value of 0.25 and ω (variable parameter that indicates the short-range interactions) with a standard value of 0.2.

$E_x^{PBE,SR}$, $E_x^{PBE,LR}$ y E_c^{PBE} are parameters used in the functional PBE (different from the worked ones) and that indicate the components at different ranges and the correlation functional respectively. Finally $E_x^{HF,SR}$ indicates the Hartree-Fock exact exchange functional of short-range.

- **Grimme's approximation**[8]

The hybrid functionals provide very accurate results in the majority of the cases and due to that reason they are the most used currently. However, there are situations where they do not fit real values, as when by the method it is obtained that the structure "a" is more stable than the structure "b", but experimentally it has been demonstrated that the situation is just the contrary. To avoid this error Grimme proposed some empiric correction values for DFT method where dispersion of energy is considered.

An example where this approximation is needed to match the experimental and theoretical value is the rutile and anatase structures, which are different forms of the TiO_2.

Table 1. Parameters of Grimme

Element	C_6	R_0	Element	C_6	R_0
H	0.14	1.001	K	10.80[c]	1.485
He	0.08	1.012	Ca	10.80[c]	1.474
Li	1.61	0.825	Sc–Zn	10.80[c]	1.562[d]
Be	1.61	1.408	Ga	16.99	1.650
B	3.13	1.485	Ge	17.10	1.727
C	1.75	1.452	As	16.37	1.760
N	1.23	1.397	Se	12.64	1.771
O	0.70	1.342	Br	12.47	1.749
F	0.75	1.287	Kr	12.01	1.727
Ne	0.63	1.243	Rb	24.67[c]	1.628
Na	5.71[c]	1.144	Sr	24.67[c]	1.606
Mg	5.71[c]	1.364	Y–Cd	24.67[c]	1.639[d]
Al	10.79	1.639	In	37.32	1.672
Si	9.23	1.716	Sn	38.71	1.804
P	7.84	1.705	Sb	38.44	1.881
S	5.57	1.683	Te	31.74	1.892
Cl	5.07	1.639	I	31.50	1.892
Ar	4.61	1.595	Xe	29.99	1.881

Real and reciprocal spaces

The concept of real space is intuitive since it is the one used daily. It is the place where objects are located and the events that happen have relative position and direction. In this real space it is possible to work with classic mechanics, which makes it ideal in the calculation for bodies of finite and measurable magnitudes.

In contrast there are the infinite bodies, whose properties imply a big amount of calculations, many times not possible to be performed. For studying these bodies it was developed an idea that allowed the representation of them with finite magnitudes, the reciprocal space.

The case dealt with in this project is based on a solid that is considered a periodic system of infinite atoms. For the calculation of some of its properties a series of mathematical operations is used, to get a group of imaginary points belonging to the reciprocal space, for crystals in 2D the Equation 24 is applied and the Equation 25 is for crystals in 3D:

$$a_i \, b_j = 2\pi \, \delta_{ij}$$

Eq. 24

$$\vec{k} = \left(\frac{2\pi m}{a_1}, \frac{2\pi n}{a_2}, \frac{2\pi q}{a_3} \right)$$

Eq. 25

Where “a” represents the vectors generators of the direct net:

$$\vec{R} = m_1 \vec{a}_1 + m_2 \vec{a}_2 + m_3 \vec{a}_3$$

Eq. 26

And “b” the ones generating the reciprocal one:

$$\vec{K} = v_1 \vec{b}_1 + v_2 \vec{b}_2 + v_3 \vec{b}_3$$

Eq. 27

Once the set of points of the reciprocal space (first zone of Brillouin) is got, calculations are easier. From the 14 different zones of Brillouin corresponding to the 14 cells of Bravais, the ones that are going to be worked are: R3m (trigonal) and P61 (hexagonal).

Equation of state (EOS)

The equations of state are thermodynamic mathematic expressions (from the more complex ones to the easiest ones) that determine state variables, which define the physic conditions of a compound as pressure, temperature, volume or the internal energy.

There are lots of EOS because each one allows to define one or more variables and furthermore they change with each different system. The equations that are going to be use in this project are the following ones:

- Murnaghan equation[9]

This EOS shows the relation between the volume of a system and the applied pressure. It bases on Boyle law but adds two variable parameters: the incompressibility module or Bulk modulus (K_0) and the first derivate of this module versus the pressure (K_0'.)

Usually those parameters are experimentally determinate giving values to P and V. The obtained EOS is:

$$P(V) = \frac{K_0}{K_0'}\left[\left(\frac{V}{V_0}\right)^{-K_0'} - 1\right]$$

Ec.28

- Birch-Murnaghan equation[10]

This EOS indicates the way that the volume of a system change while is put under pressure. It is a Murnaghan modification made by Birch three years later. The equation after the adaptation is as follows:

$$P(V) = \frac{3B_0}{2}\left[\left(\frac{V_0}{V}\right)^{\frac{7}{3}} - \left(\frac{V_0}{V}\right)^{\frac{5}{3}}\right]\left\{1 + \frac{3}{4}\left(B_0' - 4\right)\left[\left(\frac{V_0}{V}\right)^{\frac{2}{3}} - 1\right]\right\}$$

Ec.29

Grüneisen Parameter

This parameter presents, for a crystal net, the effect in vibration frequencies with a volume variation due to a rise of the temperature or pressure.

It has two different expressions, a thermodynamic one and a microscopic one. In this project is going to be applied the second one.

The microscopic expression is the combination of the thermodynamic expression with a microphysic model of vibrating atoms inside the crystal, relating the atom vibration frequency with the interaction of this atom, the direction of the applied pressure (the vector of direction and intensity of the pressure) and the other atoms. The expression is:

$$\gamma_i = -\frac{k_0}{\omega_o}\frac{\partial \omega_i}{\partial P}.$$

Ec. 30

Band structure

To introduce the concept of structure of bands first the presentation of the theory of bands is needed. By this theory, the electronic structure of a compound is described, an In_2Se_3 crystal in this project, as a structure of energy bands. This is possible since the orbitals of the atoms when joining to make a molecule overlap, producing a discreet number of molecular orbitals, each one with its own energy.

When the crystal has a big number of atoms, the number of orbitals of valence is also big and, as the energy difference is so low, the energy levels nearly overlap forming continuous bands. Among bands, empty breaches are created, due to the absence of orbitals in such energies (these breaches will be formed whatever the number of atoms may be).

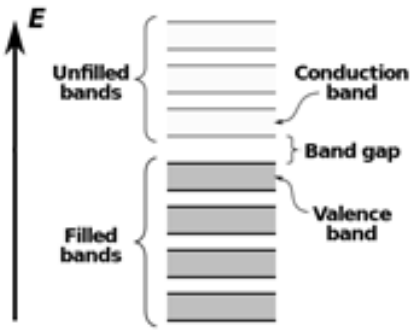

Figure 6. Bands structure representation

The band occupied by the most external electrons of the atom (the ones in the last layer) will be the valence band. These electrons are used to make bonds but they cannot be used for electrical conduction.

The conduction band is the first one that presents free electrons and the band that produces electrical conduction, since these electrons are not linked to the atoms anymore and, therefore, they can move along the crystal.

Another concept that must be considered is the one called in this work, the maximum of the valence band, the Fermi's energy or level. There is another definition of this concept widely used in solid-state physics, defined as the average between the two bands, with the conduction band that is located in the upper part of the Fermi's energy and the valence band located in the lower part.

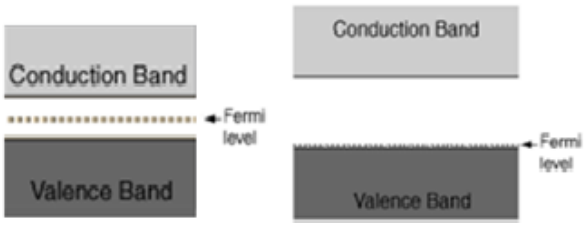

Figure 7. Two different appreciations of the Fermi level

The minimum separation between the conduction band and the valence band is called band gap and there is no energy levels in this zone. Its value is measured taking the lowest energy in the conduction band and deducting the value of the highest energy in the valence band. These values are obtained from some of the vectors in the first zone of Brillouin, in such a way that if the vector representing the maximum of the valence band and the vector representing the minimum of the conduction band are the same one, a direct gap will be given, meanwhile if different vectors represent the maximum and the minimum, the gap will be indirect. Some examples of direct and indirect gap are found in the below figure[11]:

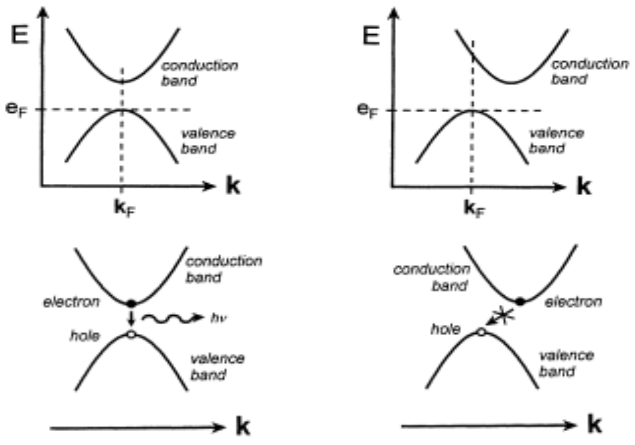

Figure 8. Direct (left) and indirect band gap (right)

It should be pointed out that the indirect gap as it is will present a very low intensity, this is because the electron need to promote to an another energy level using a special way that is not simple due to the change of the electron momentum. To make a successful transition of the electron to the valence band must be done by the assistance of lattice vibrations.

Usually, the experimental calculation of the band gap value is done by absorption spectroscopy because is an easy way to obtain it and allows to determine the kind of gap (direct or indirect) by one step. To use this method, each power will mark an absorption coefficient (α) versus energy of the photon graphic.

Analyzing the different kind of results is observed that for the direct gap α is related by the following formula with the frequency:

$$\alpha \approx A^* \sqrt{hv - E_g} \quad \text{when} \quad A^* = \frac{z^2 x_{vc}^2 (2m_r)^{3/2}}{\lambda_0 \varepsilon_0 \hbar^3 n}$$

Ec. 31

α is the coefficient of absorption, ħ is the constant of Plank, v is the frequency of the light, E_g is the energy of the band gap, A^* is a constant of independent frequency, z is the elementary charge, n is the refractive index, ε_0 is the permittivity of the vacuum, x_{vc} is a "matrix element" with units of length and values of the same order of magnitude than the constant of network and lastly m_r is represented by the following formula:

$$m_r = \frac{m_h^* m_E^*}{m_h^* + m_E^*}$$

Ec. 32

Where m_E^* and m_h^* are the effective masses of the electron and gap respectively and m_r is the reduced mass.

The formula applied to an indirect gap is:

$$\alpha \propto \frac{(hv - E_g + E_p)^2}{exp\left(\frac{E_p}{kT}\right) - 1} + \frac{(hv - E_g + E_p)^2}{1 - exp\left(-\frac{E_p}{kT}\right)}$$

Ec. 33

Where E_p is the energy of the phonon of the transition, T is the thermodynamic temperature and the other parameters have been defined for the Ec. 29

So, if it is represented α^2 versus hv and a straight line is obtained, the band gap is going to be direct and the value of the gap can be calculated when α is zero. If this step give another kind of line the graphic that is going to be plot is $\alpha^{1/2}$ versus hv. If this second graphic shows the straight line the gap is indirect and it is calculated giving to E_p and α the zero value and solving the equation.

Here below are shown the two different α graphics:

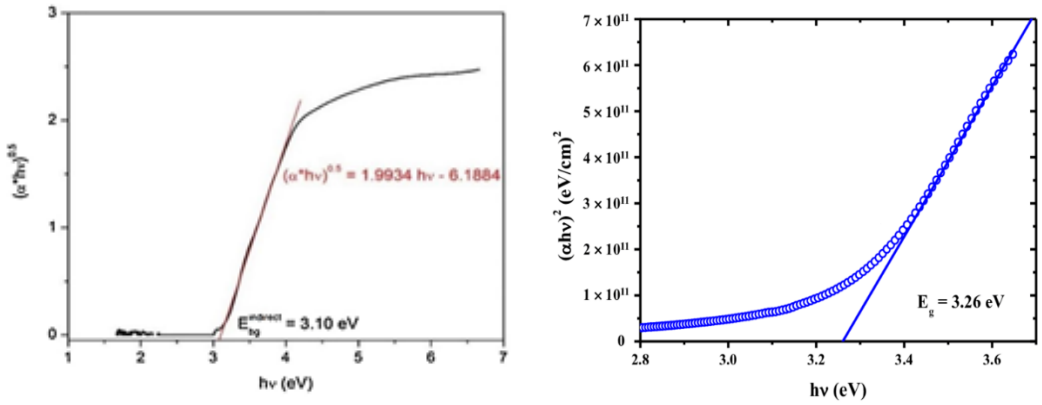

Figure 9. Representation of the absortion coefficient to direct and indirect band gap

The value of the band gap indicates the solid ability to conduct electricity, in this project is between 3 and 1 eV and can be considered as semiconductor.

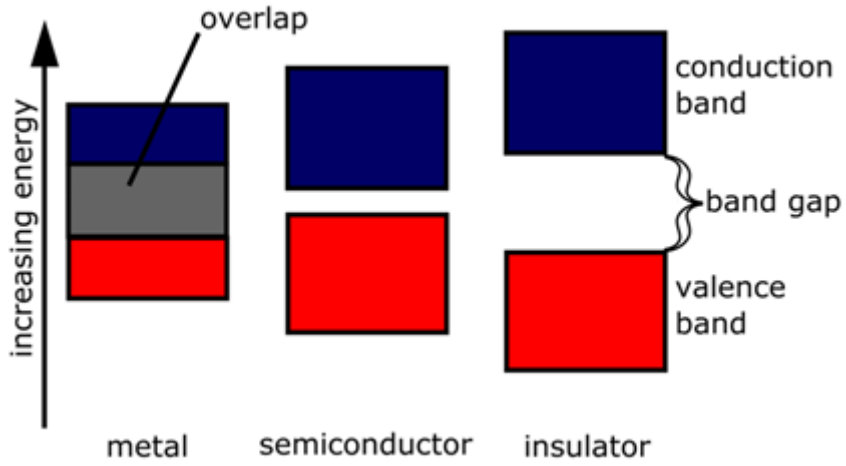

Figure 10. Different conductivities due to the band gap

Computational details

This project is done by a Linux terminal with crystal program in its crystal17 version[12]. The program allows great variety of calculations related with the solid state chemistry in 0 (molecules), 1 (linear polymers), 2 (crystal surfaces or films) and 3 dimensions (crystals). It uses as a base the calculation methods, crystallographic bases and hybrid functionals that has been introduced before.

Crystal17 takes the crystal systems as periodic, this consideration allows the simplification and the speed-up of all the calculations.

To do the calculations the program ask for four different kind of archives that are the bases for almost all the calculations of this project.

- INPUT

This archive contains the following structure for the dada: First of all there are one line for the title, the next lines indicate the type of calculation that is going to be done and the conditions (in this case the value of the pressure) and other parameters. Then comes the crystallographic bases, the order doesn't matter. And lastly comes the step, the functionals and another values as modes of work that can be found in the manual.

- OUTPUT

In this section the results of the calculations are shown, usually as a values table. Firstly is shown the time and the module of the calculation machine that have made the solution process, secondly the parameters that has been set in the INPUT. When this first part ends a resume of the equations that has been solved and all the calculation are shown. Lastly the iteration process can be found with the final solution at last.

- Fort.34 y Fort.9

Those archives are given by crystal as a complement of the optimization processes. Fort.34 gives additional information of the geometry of the structure and serve as complement in subsequent calculations. Fort.9 contains electronic structure information that can be used with a specialized program (xcrysden, crysplot or origin) to obtain the bands diagram and a band gap.

Previous data:

Once is done the introduction and set the basis of this project the experimental part begins. Then the atomic bases must be obtained, by an experimental procedure or using data bases. For this project are obtained from the Crystal17 data bases that can be seen in Annex 1.

After obtaining the atomic bases, the structural parameters are obtained from the related experimental papers, where a, b and c parameters are going to be used as bases for the optimization calculations. Those values are the following ones:

- α structure:

This structure is an R3m trigonal one (nº 160), and for this kind of structure are set the following parameters: a = b ≠ c.

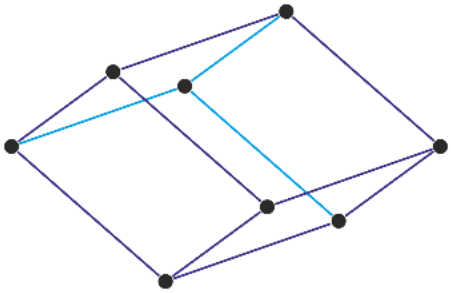

Figure 11. Primitive cell for alpha structure.

The experimental values[13] in angstroms (Å) that are going to be used are:

Table 2. α lattice parameters.

R3m	a = b	c
	4.025	28.762

Table 3. α internal coordinates

R3m	x/a	y/b	z/c	Wyckoff
In	0	0	0.5334	3a
In	0	0	0.7121	3a
Se	0	0	0.2396	3a
Se	0	0	0.8120	3a
Se	0	0	0	3a

Lastly is shown the structure obtained by the use of Diamond software[14] :

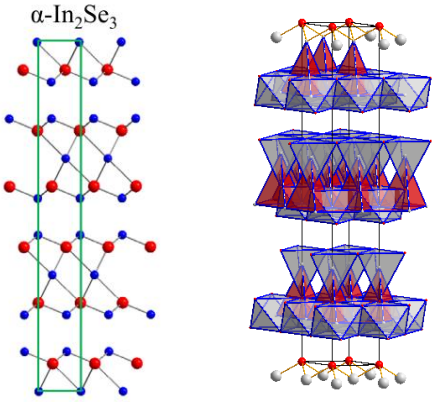

Figure 12. Experimental α structure

The α structure is set is formed by a parallel sequence of alternate layers of InSe4, SeIn4, INSe6. The Se atoms are always in a tetrahedral coordination with the In ones (red tetrahedral), whereas the In atoms have two different coordinations: InSe4 tetrahedra and InSe6 octahedra (both in blue).

- γ structure

The experimental structure is hexagonal space group (spg) P61 (nº 169). This structure establish the next conditions: a = b ≠ c and Ɣ=120º as it is shown in the Figure 13.

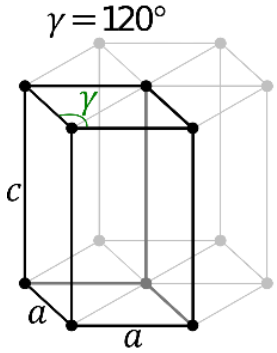

Figure 13. Primitive cell to Ɣ structure

The experimental lattice parameters (Å) and coordinates are the following ones[15].

Table 4. Ɣ lattice parameters

P61 spg 169	a = b	c
	7.1286	19.3810

Table 5. γ internal coordinades

P61	x/a	y/b	z/c	Wickoff
In	0.0117	0.3137	0	6a
In	0.3415	0.0152	0.3049	6a
Se	0.0742	0.3470	0.1470	6a
Se	0.3473	0.0436	0.1693	6a
Se	0.3662	0.0250	0.5146	6a

And finally the structure obtained by the optimization of the values:

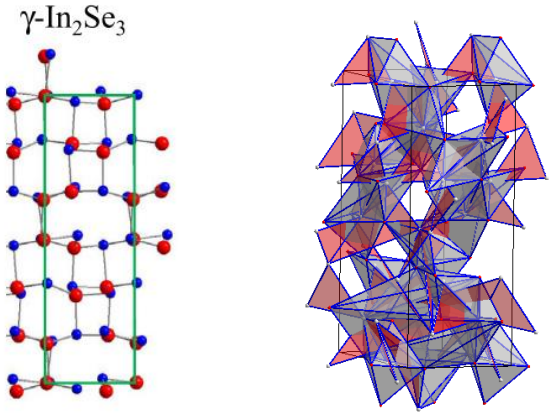

Figure 14 Experimental ϒ structure[16]

This geometry structure is more complicated than the alpha one. It is not set in layers, it has an intricate geometry that is not common in this kind of semiconductors. In this geometry each Se atom has three In atoms circling it (red) in a triangular geometry. The In (blue) form five-fold coordinated polyhedra.

Stability criteria:

In order to check which of both structures present the best stability when the pressure rises this work will follow three different stability criteria.

- The first one is the energy minimization or convergence criteria.

Is considered that a structure is stable when the first derivate of the energy front the coordinates is equal to zero. The coordinates are the ones that are going to be optimized (q_i).

$$\frac{dE}{dq_i} = 0$$

- Second criteria is the dynamic criteria

To ensure that the optimized structure is a true minima it is necessary that all the second derivatives of the energy with respect to the coordinates are positive.

$$\text{all } \frac{d^2E}{dq_i^2} > 0 \longrightarrow \text{stable} \quad \text{, one or some } \frac{d^2E}{dq_i^2} < 0 \longrightarrow \text{metastable}$$

Where q_i are the cell and internal parameters to be optimized

Furthermore as the frequency values are equal to the second derivate of the energy front q, this condition is equivalent to that all the frequency vibrations are positives.

The results for each pressure are going to be compared with the values of the lower pressures and if the vibration frequency has decreased means that there is an instability and the structure is trying to transform in other one. If the values of the frequency increase with the pressure the structure is stable.

- The third criteria is the elastic one:

After the calculation of the elastic constants, the matrix are check in order to ensure that the obtained values fulfill the adequate relations of each structure. If the results obey this relations the structures are elastically stable but if one of the relations is not fulfill it represents an instability in the structure.

Next are show the standard parameters of each structure:

Table 6. Trigonal elastic constants matrix

C_{11}	C_{12}	C_{13}	C_{14}	C_{15}	0
	C_{11}	C_{13}	$-C_{14}$	$-C_{15}$	0
		C_{33}	0	0	0
			C_{44}	0	$-C_{15}$
				C_{44}	C_{14}
					C_{66}

Table 7. Elastic stability relations for a trigonal structure.

C_{44}	>0
$C_{11}-\lvert C_{12}\rvert$	>0
$C_{13}^2 - ½C_{33}(C_{11}+C_{12})$	<0
$C_{14}^2+C_{15}^2 - ½C_{44}(C_{11}-C_{12})$	<0

Table 8. Hexagonal elastic constants matrix

C_{11}	C_{12}	C_{13}	0	0	0
	C_{11}	C_{13}	0	0	0
		C_{33}	0	0	0
			C_{44}	0	0
				C_{44}	0
					C_{66}

Table 9. Elastic stability relations for a hexagonal structure

C_{44}	>0
$C_{11}-\|C_{12}\|$	>0
$2 \cdot C_{13}^2 - C_{33}(C_{11}+2 \cdot C_{12})$	<0
or	
$2 \cdot C_{13}^2 - C_{33}(C_{11}+C_{12})$	<0

In addition of these three criteria, two more studies are going to be made to ensure that the results are reliable.

- The EOS study.

To use this method is necessary to calculate the EOS for each structure and pressure, then is graphically represented the given values in atomic units of free energy of Gibbs (G) or enthalpy (H) versus the pressure in GPa. Two different solutions can be obtained by doing this representation: the first one is that both structure line representations don't cross at any point, so the structure which have the bottom line is in the studied pressures more stable than the other one; and the second one is that the lines cross, that means that the structure line form the bottom (which was the most stable) now comes to the upper side becoming the less stable. This is an example of two crossing lines:

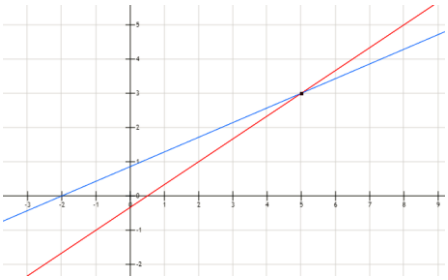

Figure 15. Crossing point example

In this case the red structure is more stable than the blue one since the pressure arrives to 5 GPa, after that point the blue one is going to be the most stable.

- Band structure and band gap (Eg)

If the band structure evolution is studied, irregularities can be detected. The most important irregularities that can be found is the change of the band gap type, from direct to indirect or vice versa and a change in the band gap values dynamic

As a experimental examples those band diagrams are shown:

Hexagonal:

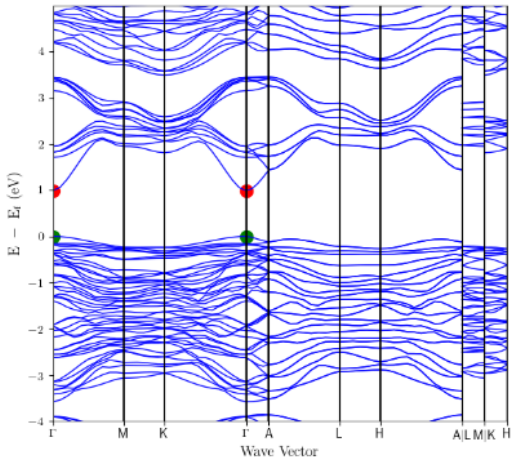

Figure 16. Experimental band structure for hexagonal structure [16]

Trigonal:

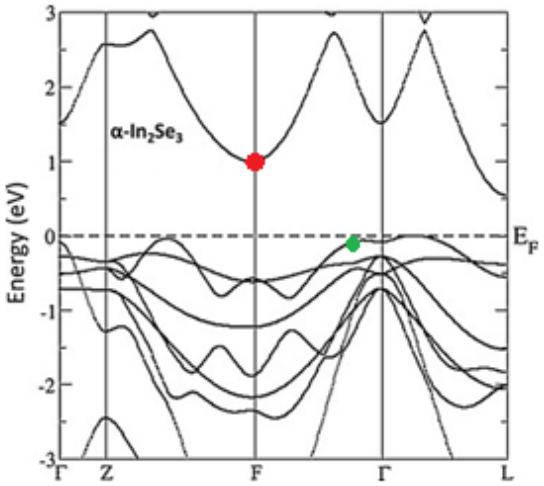

Figure 17. Experimental band structure for trigonal structure[17]

Results and discussion:

Here bellow are shown the results of the different calculations and its interpretation.

Here are represented the values of the lattice parameters at ambient pressure for the functionals B3LYP-D3 and HSE06 to choose the best one to use in this project.

Table 10: Comparation of Experimental values and optimized one for each structure

R3m	a =b	c	**P61**	a = b	c
Experimental	4.02	28.76	Experimental	7.13	19.38
B3LYP-D3	4.06	28.18	B3LYP-D3	7.21	18.91
HSE06	4.08	28.10	HSE06	7.22	18.89

As the optimized B3LYP-D3 values adapt better to the experimental values all the calculations are going to be done using this method.

The following table shows the volume and lattice parameters changes under the determined pressures for the two different structures.

Table 11: Obtained lattice parameters, volume and energy for α structure

R3m	Pressure (GPa)	a = b (Å)	c (Å)	Volume (Å^3)	E (AU)
	0	4.06	28.18	401.93	-1.868948E+04
	5	3.97	27.30	371.97	-1.868934E+04
	10	3.89	26.82	351.79	-1.868920E+04
	15	3.83	26.48	335.94	-1.868907E+04
	20	3.77	26.25	323.12	-1.868894E+04
	22	3.75	26.17	318.55	-1.868889E+04
	24	3.73	26.11	314.28	-1.868884E+04
	26	3.71	26.06	310.28	-1.868879E+04
	28	3.69	26.01	306.44	-1.868875E+04
	30	3.67	25.98	302.71	-1.868870E+04

Table 12: Obtained lattice parameters, volume and energy for ϒ structure

P61	Pressure (GPa)	a = b (Å)	c (Å)	Volume (Å^3)	E (AU)
	0	7.21	18.91	851.84	-1.121369E+05
	5	7.04	17.65	758.15	-1.121359E+05
	10	6.89	17.20	708.04	-1.121351E+05
	15	6.79	16.89	673.46	-1.121343E+05
	20	6.69	16.65	645.71	-1.121335E+05
	22	6.66	16.55	636.19	-1.121333E+05
	24	6.63	16.48	627.19	-1.121330E+05
	26	6.60	16.39	618.75	-1.121327E+05
	28	6.58	16.32	611.00	-1.121324E+05
	30	6.55	16.25	603.77	-1.121321E+05

The volume values decrease under pressure.

After an optimization of the structure, the second order Birch-Murnaghan EOS are calculated. The obtained values are represented, first of all the Energy in front the pressure, then the free energy of Gibbs; and the graphics that are procured are check to know the stability of the compound:

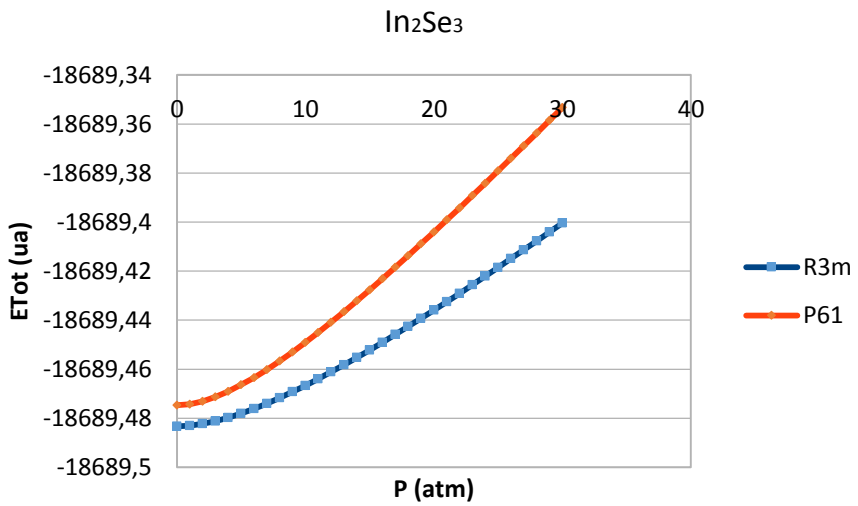

Figure 18 Energy vs pressure representation of the two structures

As it can be noted both structures achieve a minimum at the pressure value equal to zero. This result means that the two structures will be stables.

After this step a new graphic is done using the Gibbs values in all the pressure range. By this plot is check if there are any intersection between the structures.

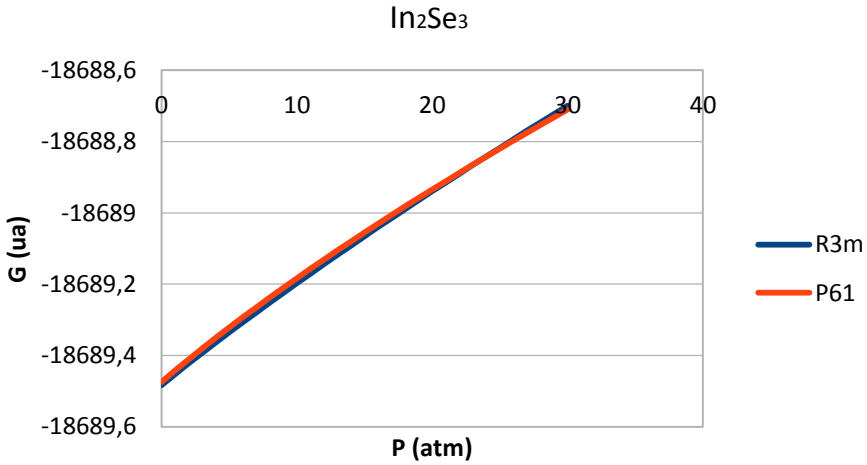

Figure 19. Free Gibbs energy vs pressure

As the graphic is not really easy to read, due to the proximity between the two structure values, the next chart try to make easier to determine the cut point of the lines. To achieve an easy way to find the intersection point is represented the free energy of each structure minus the free energy of one of them (in this case is chosen the P61 free energy). Doing this P61 structure is going to be the abscissa axis and the R3m structure is going to become positive after the cut point.

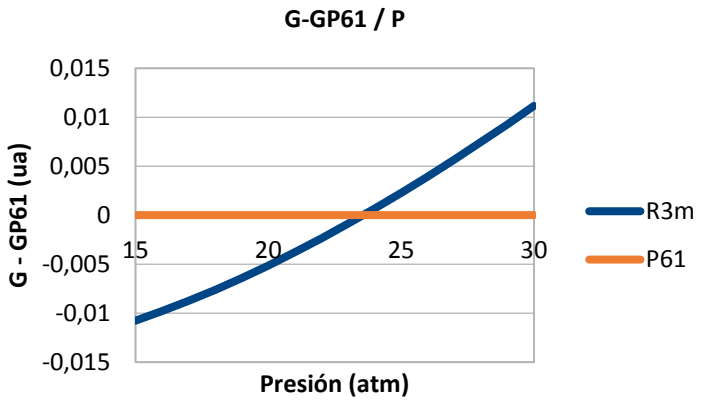

Figure 20. Both structures G minus the G P61 to obtain a clear intersection point

The graphic shows that there is a pressure induced phase transition at 22 GPa. In order to check this results the second criteria is the next one.

Once the EOS are solved the value of the bulk modulus[18] (K_0) and the first derivate (K_0') are obtained for each structure. For α, the values are K_0=52.71GPa and K_0'=5.33, for ϒ are K_0=33.54GPa and K_0'=3.79. This values indicate that the γ phase is more compressible that the α one.

Vibration frequencies:

For the frequencies, the alpha structure presents 15 vibration modes (Γ = 5E+5A) and the frequency values of alpha structure in cm^{-1} are set on the next table.

Table 13.Trigonal frequency values in cm^{-1}:

Mode\Pressure (GPa)	0	5	15	20	22	mode	24	26	28	30
E	0.0	0.0	0.0	0.0	0.0	E	0.0	0.0	0.0	0.0
A	0.0	0.0	0.0	0.0	0.0	A	0.0	0.0	0.0	0.0
E	36.2	39.4	40.8	41.0	40.5	E	40.3	39.7	39.2	38.6
E	103.4	115.2	133.3	140.7	144.0	E	146.9	149.4	151.4	153.7
A	121.6	137.5	160.9	170.6	174.2	A	177.8	180.9	184.0	187.2
E	178.0	193.1	215.4	224.6	227.9	E	230.8	233.2	235.9	238.3
A	187.1	198.5	218.6	227.7	231.4	A	235.1	238.4	242.0	245.2
A	210.6	224.2	248.0	258.9	263.2	E	266.9	269.3	271.6	274.2
E	211.0	228.7	251.9	261.0	264.2	A	267.3	271.1	275.3	279.3
A	268.3	286.1	318.9	332.8	338.2	A	343.4	348.8	353.6	357.8

The second E value evolution increase until 22 GPa and then start decreasing. This behavior shows an instability of the alpha structure at that pressure and match with the result obtained by first criteria. Here a graphic that shows the values of the irregular E vibration:

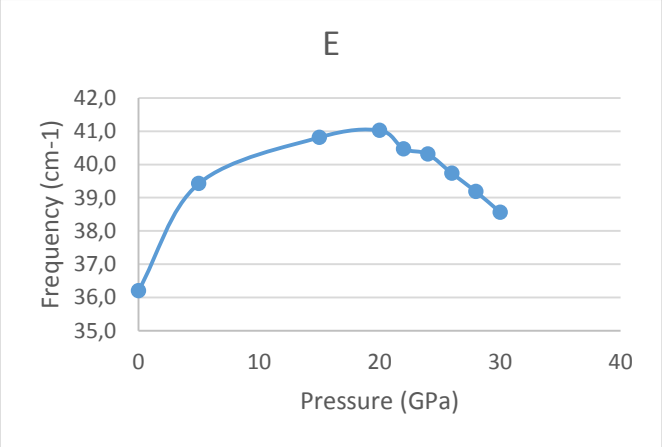

Figure 21. Evolution of the soft phonon E (red one) in the pressure range.

And then the Grüneisen parameter for this E is calculated from 0 GPa to 20 and from 22 to 30:

Υ (0-20) = 0.35
Υ (22-30) = -0.31

The Grüneisen parameter indicates, passing from positive to negative, what is seen in the figure 21, the change in the slope above 22GPa.

For γ structure there are 75 vibration modes (Γ =15E_1+15E_2+15A) active in Raman. As the quantity of values is too big the table is not going to be presented. The results shows, with little variations, that this structure is stable in all the studied pressure range.

Band structure.

The obtained files fort.9 of each pressure are used to get all the different band structures. To do it is necessary a specific software, the xcrysden [19], which allow the transformation of the fort.9 values into a band structure by calculations, related on the first Brillouin zone k points and vectors that link those.

Alpha (R3m):

The generator vectors that are obtained from the representation of the first Brillouin zone are the next ones:

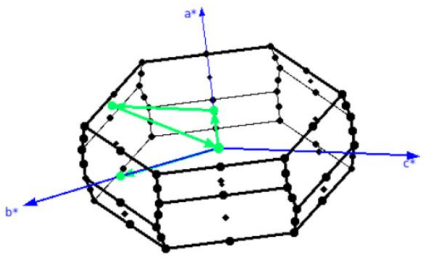

Figure 22. Trigonal first Brillouin zone and the k vectors used to do the band structure

And the band structure (with the Fermi level as the top of the valence band in red):

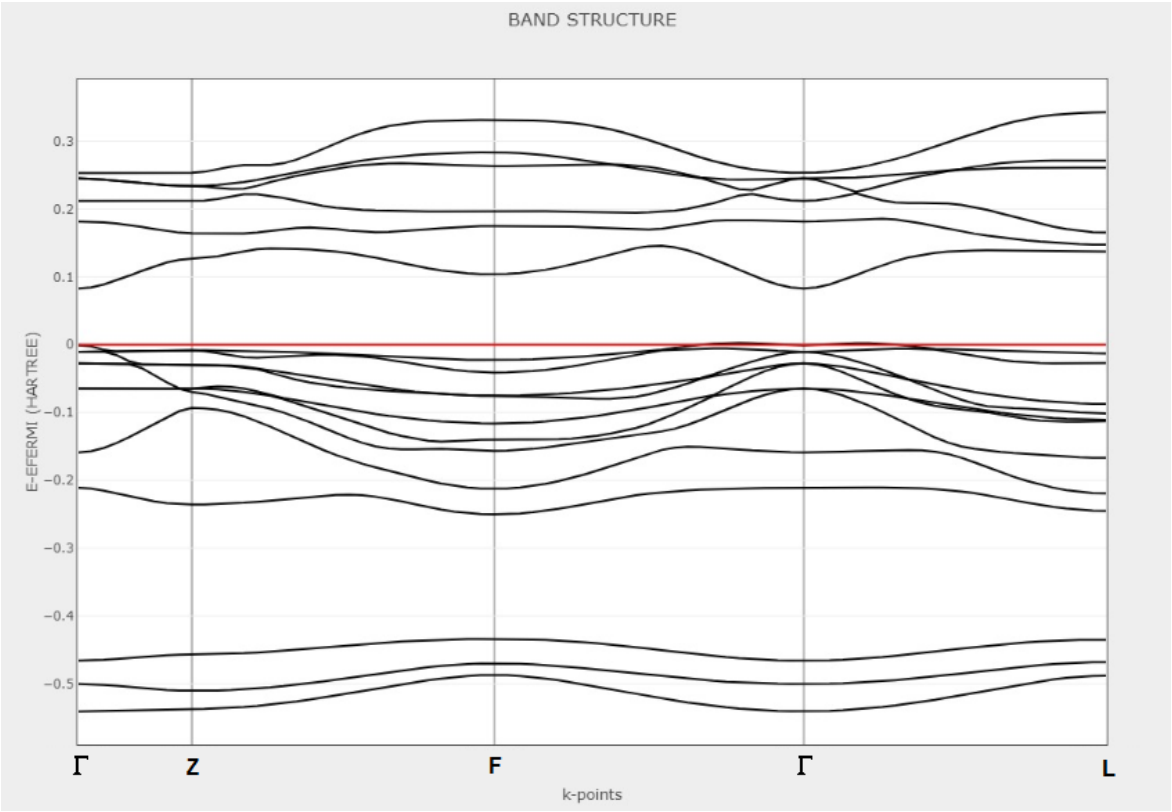

Figure 23. α band structure for direct gap

When the pressure reach the 22 GPa there is a change in the band gap and this is shown in the following band structure for the 24 GPa (the change is clearer at this pressure):

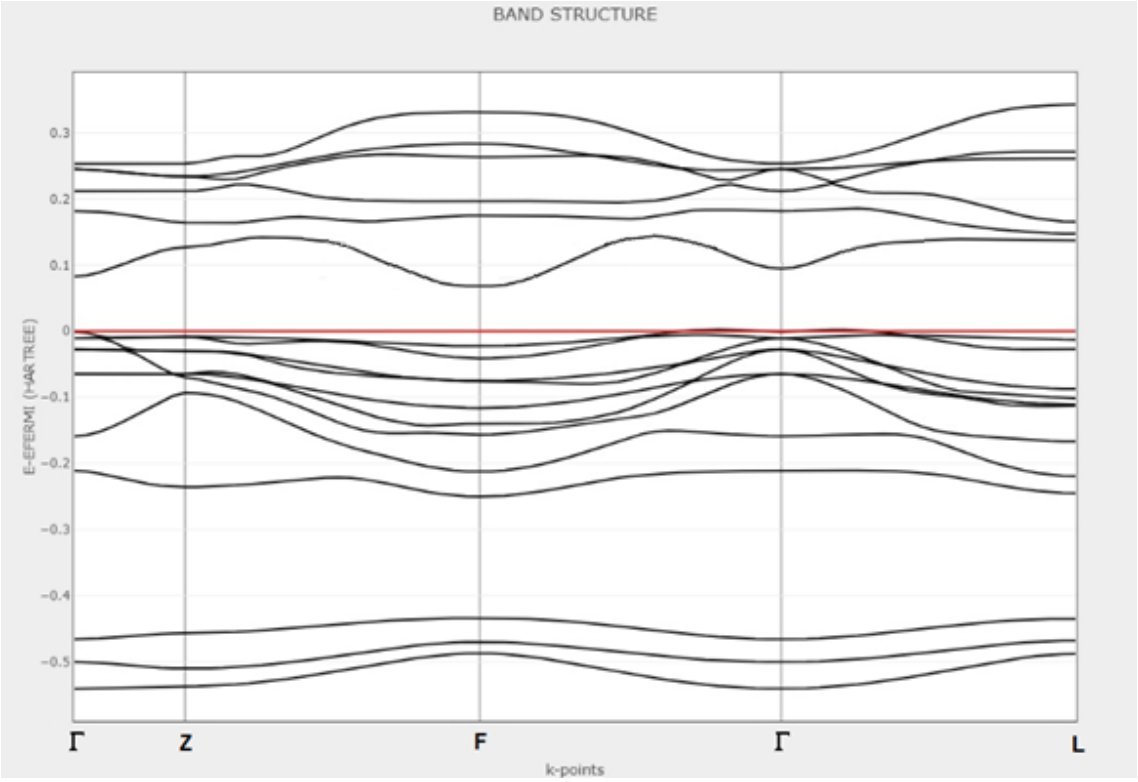

Figure 24. α band structure for indirect gap

As can be seen the band gap is indirect at this pressure and goes from the Γ point to the F (1/2.1/2.0) point.

At the same time than the structure band is calculated the band gap (Eg) is obtained too and its evolution is plot here:

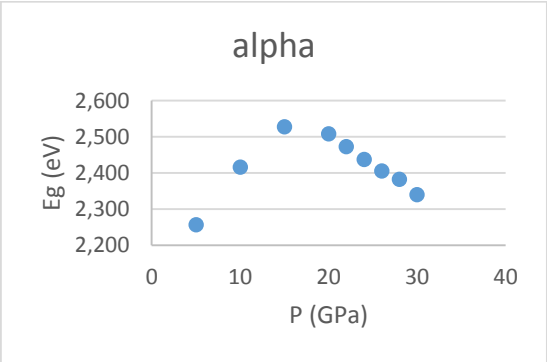

Figure 25. Evolution of the band gap with the pressure

The band gap increases since 20 GPa and then start to decrease when increase the pressure. Furthermore, when the pressure is around 20 GPa the evolution of the band gap changes and the kind of the band gap changes too. First it is a direct gap $\Gamma \rightarrow \Gamma$ and after the indicated pressure is an indirect gap $\Gamma \rightarrow$ F (1/2.1/2.0)

The density of states (DOS) describes the number of states that are available to be occupied by the system at each level of energy. For α structure there is two different In atoms and three Se atoms, as the values are similar in one hand for the two In atoms and in the other hand for all the Se atoms, the results are shown as the addition of all the In values in the upper graphic, the Se in the middle and the total at the bottom. Those graphics are shown here bellow:

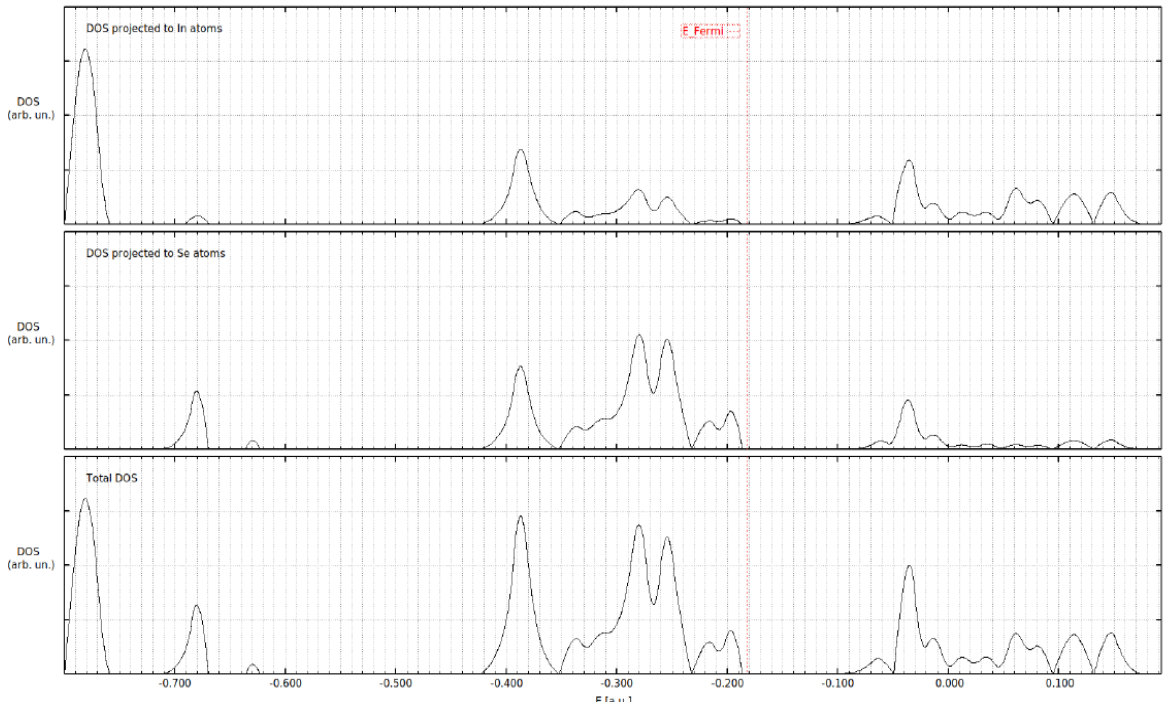

Figure 26. α DOS

The diagram shows that the top of the valence band is occupied by Se 4p electrons and the most internal bands are occupied by In 5p and 5s electrons. The bottom of the conduction band is occupied by both of the atom electrons equally.

Then the hydrostatic band gap deformation potential[20], which is defined as the multiplication of the bulk modulus per the derivate of the band gap with respect to the pressure($a_g = -K_0 \cdot \frac{dE_g}{dP}$), has been calculated:

$a_{g(0\text{-}20)}$ = - 0.66 eV

$a_{g(20\text{-}30)}$ = 0.70 eV

As can be seen in the values there is a tendency change at around 20 GPa, passing from a negative value to a positive one. Furthermore is the pressure at which the band gap changes from direct to indirect.

Gamma:

To this structure the same steps are followed, first the Brillouin zone and the generator vectors:

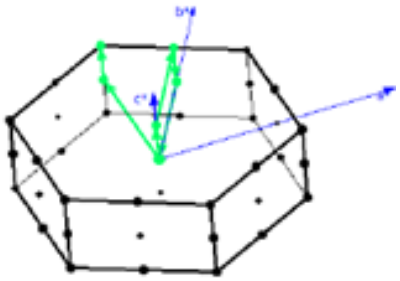

Figure 27. Hexagonal first Brillouin zone and the k vectors used to do the band structure

Then the structure band with the Fermi level:

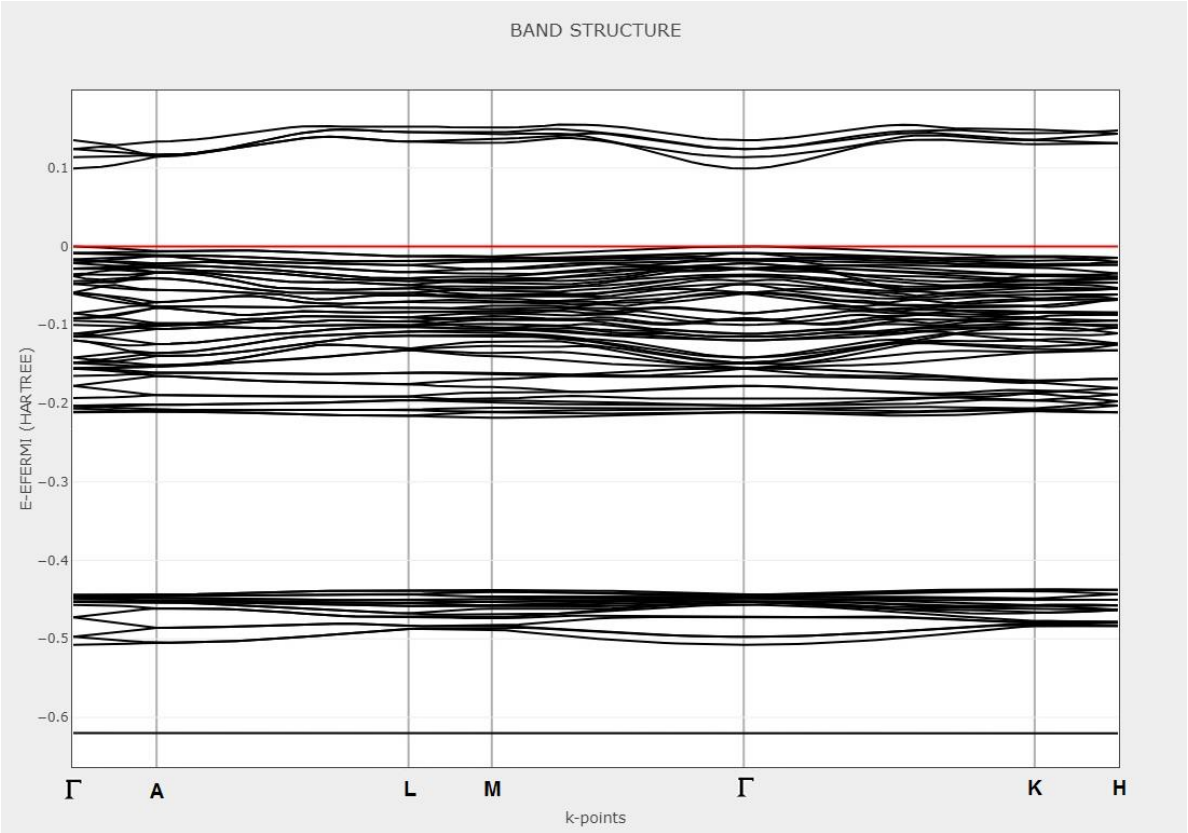

Figure 28. Υ band structure

At ambient pressure the gap is direct $\Gamma \rightarrow \Gamma$ as can be seen in the previous figure. However the other band gaps must be analyzed too because it can change as it happens in the α structure.

Before checking the band gap evolution the DOS of the γ structure is presented in the same way that the α DOS.

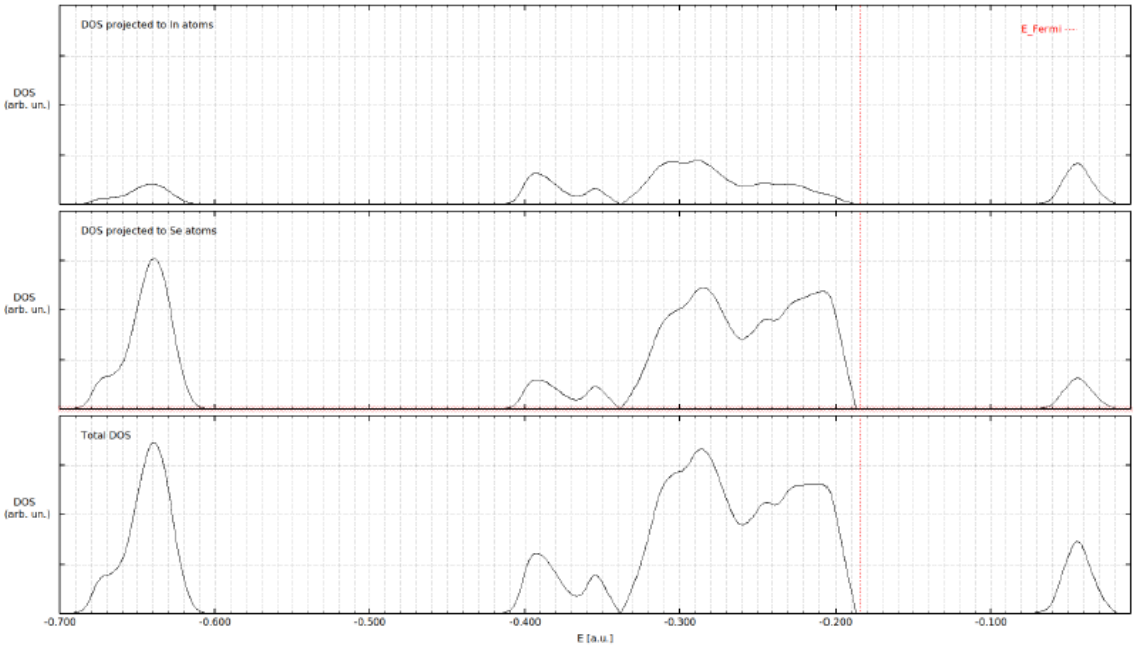

Figure 29. γ DOS

Is observed that all the contributions are made by the selenide (second picture).

And finally the evolution of the band gap with pressure in the next graphic:

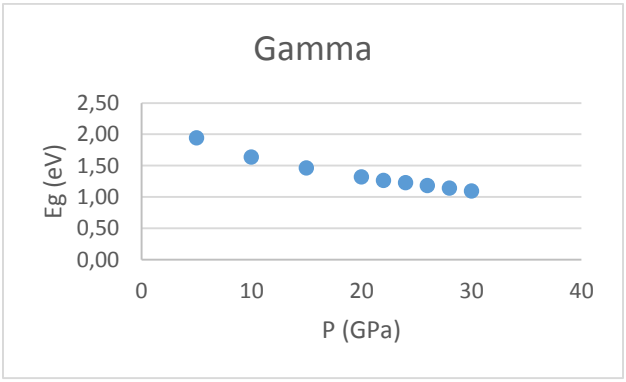

Figure 30. Evolution of the band gap with the pressure

The band gap decreases with increasing pressure and in this case do not suffer changes and it remain in all the pressure range as a direct gap $\Gamma \rightarrow \Gamma$

The calculated band gap deformation potential is:

$a_{g(0\text{-}30)}$ = 0.95 eV

The value of a_g of γ structure is higher than the value of α structure. This indicates that the γ gap will compress more with the increasing pressure than the α one.

Elastic constants:

The elastic constants are obtained for each structure and pressure. Here bellow the two matrices with the elastic constants got at 1 GPa pressure are shown as representative of the full set of pressure.

Before the elastic constant matirces are presented the conditions of the phase, those are: K or Bulk modulus which has been defined yet, G or shear modulus that is defined as the ratio of shear stress to the shear strain, E or Young modulus which is a mechanical property that measures the stiffness of a solid material and ν or Poisson ratio that is defined as the negative of the ratio of transverse strain to axial strain.

For the trigonal phase:

Table 14.Mean conditions of the trigonal phase

P=0	K	G	E	ν
GPa	53.13	21.42	56.64	0.322

Table 15. Trigonal elastic constants matrix at ambient pressure

Cij	1	2	3	4	5	6
1	99.257	42.685	30.821	0	0.042	0
2		99.257	30.821	0	-0.042	0
3			77.489	0	0	0
4				14.048	0	-0.042
5					14.048	0
6						28.286

Table 16. Elastic constant relations

C44	14.048	>0
C11-|C12|	56.572	>0
$2C13^2$-C33(C11+2C12)	-12406.6935	<0

For the hexagonal phase:

Table 17. Mean conditions of the hexagonal phase

P=0	K	G	E	ν
GPa	37.03	17.51	45.37	0.296

Table 18. Hexagonal elastic constants matrix at ambient pressure

Cij	1	2	3	4	5	6
1	67.387	34.847	20.763	0	0	0
2		67.387	20.763	0	0	0
3			52.489	0	0	0
4				17.47	0	0
5					17.47	0
6						16.27

Table 19. Elastic constant relations

C44	17.47	>0
C11-|C12|	32.540	>0
$2C13^2$-C33(C11+2C12)	-6333.04027	<0
$2C13^2$-C33(C11+C12)	-4503.95609	<0

Only the 1 GPa pressure matrices are shown because the other ones fulfil the stability parameters too and it is unnecessary to present all the values here.

Conclusion:

In this project, the dynamic and the elastic stability criteria has been studied for analyzing the pressure induced phase transition between the alpha and gamma phases. With the results that have been shown, following the explained different criteria, can be concluded that α and γ structures presents elastic stability in all the range of studied pressures because all the elastic constant standards are fulfill.

Both structures are elastically stables but α presents a dynamic instability at around 22 GPa. This instability can be proved by the study of the frequencies, where the soft phonon E grows since 22 GPa and then decrease. It can be proved too analyzing the intersection in the Free Gibbs energy vs pressure where cut at around 22 GPa the γ structure line becoming less stable than the second one. The last studied parameter is the band structure, which confirm the 22 GPa instability because the transition of the direct band gap to indirect is at this pressure and the band gap increases since this pressure too and then decrease.

γ structure shows different results for each analysis. The dynamic criteria shows instability at low pressures, that stabilize at 22 GPa. The Gibbs graphic shows that at 22 GPa the γ structure becomes more stable than α one. Lastly the band gap do not change in all the pressures range so there is not instability in this way.

Using those results can be determined that the transition between the two phases happens by a dynamic process, not an elastic one when a 22 GPa pressure is applied. This fact has been demonstrated by the tendency change of the E_g at around 20 GPa, where the gap pass from direct to indirect too. Furthermore, this gap change can indicate that the transition between the two phases may be related with an electronic effect.

Additionally, as a personal conclusion, this project has helped me to learn how to use different programs such as Crystal, Xcrysden , Diamond, Crysplot… which maybe I would never have used if this opportunity had not appeared. I have learnt the importance of good mates who supported me when needed and the particular value of having a professional tutor guiding me in the right way and helping me as much as he could.

Bibliography:

[1] Changxi Zheng et al “Room temperature in-plane ferroelectricity in van der Waals In2Se3” *Sci.Adv* (2018), 4.

[2] Nam-Oh Kim et al “Electrical and Optical Properties of α-In2Se3 Single Crystals with an Indium Excess” *Journal of the Korean Physical Society* (2001), 38, 4, 405-408.

[3] Yu Zhou et al “Out-of-Plane Piezoelectricity and Ferroelectricity in Layered α-In2Se3 Nanoflakes” *Nano Lett.* (2017), 17, 5508−5513.

[4] M. D. Yang et al “Structural and Optical Characteristics of γ-In_2Se_3 Nanorods Grown on Si Substrates” *Journal of Nanomaterials* 2011, Article ID 976262, 5 pages.

[5] Seong Man Yu et al “The Effect of Pressure and Growth Temperature on the Characteristics of Polycrystalline In2Se3 Films in Metal Organic Chemical Vapor Deposition” *Electronic Materials Letters* (2012), 8, 3, 245-250.

[6] Becke. A.D “Density-Functional Thermochemistry. The Role of exact Exchange.” *J. Chem. Phys*. (1993), 98, 5648.

[7] Krakau. A.V. et al “Influence of the exchange screening parameter on the performance of screened hybrid functionals.” *J. Chem. Phys.* (2006), 125, 22410610,1063/1.2404663

[8]Grimme.S. “Semiempirical GGA-type density functional constructed with a long-range dispersion correction.” *J. Comput. Chem.* (2006), 27, 1787.

[9]http://www.theochem.unito.it/crystal_tuto/mssc2013_cd/tutorials/eos/eos_tut.html

[10] Birch. F. “Elasticity and constitution of the Earth’s interior.” *J. Geophys. Res.* 1952, 57, 227-286

[11] Dong-Kyun Seo and Roald Homann “Direct and indirect band gap types in one-dimensional conjugated or stacked organic materials” *Theor. Chem. Acc*. (1999), 102, 23-32

[12] R.Dovesi et al Crystal User’s manual. (2017)

[13] Jinggeng Zhao and Liuxiang Yang “Structure Evolutions and Metallic Transitions in In2Se3 Under High Pressure” *J. Phys. Chem.* (2014), 118, 5445−5452

[14] http://www.crystalimpact.com/diamond/Default.htm

[15]Han G et al “Indium selenides:structural characteristics. synthesis and their thermoelectric performances” *Small* (2014), 10, 2747-2765

[16]http://www.uam.es/departamentos/ciencias/quimica/aimp/luis/Docencia/QFES/Curso_2005-06/QFES_Ecuaciones_de_Estado_bn.pdf

[17] https://materialsproject.org/materials/mp-612740/

[18] Birch. F. “Finite Strain Isotherm And Velocities For Single-Crystal And Polycristalline NaCl At High-Pressures And 300-Degree-K.” *J. Geophys. Res.* (1978), 83, 1257

[19] A.Kokalj “J.mol graph” *Model.* (1999) , 17, 176-179

[20] Schweitzer. C.; Reimann. K.; Steube. M. *Solid State Commun.* (1999), 110, 697.

Crystal-Basis set library: http://www.crystal.unito.it/basis-sets.php

ICSD- FIZ Karlsruhe: http://www2.fiz-karlsruhe.de/icsd_home.html

Anex 1

In: In_9763111-631_Rothballer_2013

```
49 10
0 0 9 2.0 1.0229
   3806666.0     0.0000487
    565677.0     0.000386
    122672.0     0.00225
     31208.0     0.0112
      8973.58    0.0464
      2855.32    0.1551
      1009.92    0.3512
       400.013   0.427
       167.569   0.1887
0 1 7 8.0 1.0262
     11017.4    -0.00033  0.00104
      2546.93   -0.00642  0.00957
       778.611  -0.0539   0.0566
       275.526  -0.1475   0.2171
       110.525   0.1374   0.4533
        50.5711  0.6125   0.4345
        24.3037  0.4209   0.1836
0 1 6 8.0 1.0314
       239.102   0.00648 -0.0146
        92.7375 -0.0325  -0.0705
        39.0152 -0.3244   0.0317
        17.4499  0.0117   0.8767
         8.1698  0.9158   1.2929
         3.9132  0.4324   0.441
0 3 6 10.0 1.0
       342.52    0.0128
       102.01    0.0894
        38.0838  0.2915
        15.6905  0.4663
        6.77     0.3293
        2.7107   0.0554
0 1 3 8.0 1.0
        6.5969  -4.5838  -0.0762
        3.1744   1.9149   0.5664
        1.4127   9.9244   0.8942
0 1 1 3.0 1.0
        0.6351   1.0      1.0
0 3 3 10.0 1.0
        5.0783   0.1939
        1.9711   0.5072
        0.7589   0.4477
0 3 1 0.0 1.0
        0.315   1.0
0 1 1 0.0 1.0
        0.285   1.0      1.0
0 1 1 0.0 1.0
        0.14   1.0      1.0
```

Se: Se_m-pVDZ-PP_Heyd_2005

```
234 9
INPUT
24. 0 2 4 6 2 0
 30.046990 370.122888 0
 6.918688 10.456168 0
 45.773014 99.135059 0
 45.294642 198.292483 0
 20.739648 28.338747 0
 20.028601 56.749747 0
 50.941768 -18.526556 0
 49.594740 -28.334921 0
 16.323522 -0.696089 0
 14.465196 -1.167891 0
 3.775330 0.041443 0
 3.501953 0.235583 0
 11.950867 -0.766262 0
 17.810780 -2.102742 0
0 0 6 2. 1.
       2609.72040         0.182900000E-02
       391.522800         0.970600000E-02
       48.2893000         0.716060000E-01
       16.8019000        -0.383980000
       3.51490000         0.691926000
       1.58940000         0.491893000
0 0 6 2. 1.
       2609.72040        -0.694000000E-03
       391.522800        -0.386600000E-02
       48.2893000        -0.248390000E-01
       16.8019000         0.140207000
       3.51490000        -0.342280000
       1.58940000        -0.364598000
0 0 1 0. 1.
      0.383000000          1.00000000
0 0 1 0. 1.
      0.139900000          1.00000000
0 2 6 6. 1.
       100.019200         0.476100000E-02
       25.8909000        -0.848990000E-01
       6.20930000         0.428655000
       2.66130000         0.543060000
       1.09290000         0.149283000
      0.359700000         0.107100000E-02
0 2 6 4. 1.
       100.019200        -0.105800000E-02
       25.8909000         0.217090000E-01
       6.20930000        -0.126243000
       2.66130000        -0.193545000
       1.09290000         0.473730000E-01
      0.359700000         0.591806000
0 2 1 0. 1.
      0.113700000          1.00000000
0 3 6 10. 1.
       128.508000         0.110110000E-01
       41.5212000         0.778560000E-01
       15.5182000         0.232819000
       6.16082000         0.401788000
       2.41134000         0.408946000
      0.871936000         0.168093000
0 3 1 0. 1.
      0.365600000          1.00000000
```